RSC Advances

This is an *Accepted Manuscript*, which has been through the Royal Society of Chemistry peer review process and has been accepted for publication.

Accepted Manuscripts are published online shortly after acceptance, before technical editing, formatting and proof reading. Using this free service, authors can make their results available to the community, in citable form, before we publish the edited article. This *Accepted Manuscript* will be replaced by the edited, formatted and paginated article as soon as this is available.

You can find more information about *Accepted Manuscripts* in the **Information for Authors**.

Please note that technical editing may introduce minor changes to the text and/or graphics, which may alter content. The journal's standard **Terms & Conditions** and the **Ethical guidelines** still apply. In no event shall the Royal Society of Chemistry be held responsible for any errors or omissions in this *Accepted Manuscript* or any consequences arising from the use of any information it contains.

ARTICLE

Unprecedented Inhibition of Glycosidase-Catalyzed Substrate Hydrolysis by Nanodiamond-Grafted *O*-Glycosides

Aloysius Siriwardena,[a,*] Manakamana Khanal,[b] Alexandre Barras,[b] Omprakash Bande,[a] Teresa Mena-Barragán,[c] Carmen Ortiz Mellet,[c,*] José Manuel Garcia Fernández,[d,*] Rabah Boukheroub,[b] and Sabine Szunerits [b,*]

We report herein the unprecedented finding that α-*O*-glucosides and also α-*O*-mannosides, when conjugated on nanodiamond particles (ND) are not only stable towards the hydrolytic action of the corresponding matching glycosidases, but are also endowed with the ability to inhibit them. Moreover, conjugation of the *O*-glycosides to ND (glyco-ND) sees them transformed into inhibitors of mismatching enzymes (for which they do not serve as substrates even when in their monovalent, free form). The effects of the glyco-NDs have been demonstrated on a panel of commercial glycosidases and the inhibition found to be competitive and reversible and not to be related to any denaturation of enzymes by the ND-conjugates. Values for K_i in the low micromolar have been measured for certain glyco-ND (for example, a K_i value of 5.5 ± 0.2 μM was measured for the glyco-ND against the α-glucosidase from baker's yeast) and found to depend on both the identity of the enzyme and the glyco-ND. The latter K_i value compares well with that obtained for the natural glucosidase inhibitor, 1-deoxynojirimycin (K_i of 25 μM against the α-glucosidase from baker's yeast under identical assay conditions). The monovalent control *O*-glycosides were hydrolysed efficiently by the appropriate glycosidase. Glyco-ND bearing 50% loading of *O*-glycoside as well ND conjugated with both *O*-glucosides and *O*-mannosides (mixed) have also been assayed and shown also to inhibit the panel of glycosidases with potencies and selectivities different from those recorded for the 100% loaded ND and also from one another. The impact on factors such as glycotope density and heteromultivalency on inhibition is reminiscent of that typically encountered in carbohydrate-lectin recognition events. The abilities of the glyco-ND to bind, cross-link and aggregate concanavalin A, a lectin known to recognize both α-*O*-D-mannosides and α-*O*-D-glucosides, was assessed by a range of methods including an enzyme-linked lectin assay (ELLA), a two-site sandwich ELLA and a turbidimetry assay, respectively and indeed seen to reflect their expected *per glycotope* affinity enhancements as compared to monovalent controls: the high avidity of the lectin for each respective glycosylated ND particle was consistent with the manifestation of potent multivalent effects driving lectin recognition and binding.

1. Introduction

A considerable amount of effort has been devoted to studying the principles governing the interactions of natural glycans and their synthetic mimetics with glycan-specific protein partners (lectins).[1] This has demonstrated that the multivalent presentation of a particular glycotope on an appropriate scaffold (i.e. cell-membrane, dendrimer, polymer, nanoparticle, etc.) can affect significantly its potency and selectivity of binding with a given target protein, relative to that of a monovalent counterpart.[2-13] Indeed, the promise that specific lectin-mediated processes (i.e., pathogen recognition, viral entry, tumor migration and metastasis events, etc.) might be effectively modulated with a properly tailored multivalent ligand continues to see innovative glycoedifices proposed in the hope of obtaining effective carbohydrate-based therapeutics.[14] In contrast, much less effort has been consecrated to unravelling the principles underpinning interactions of natural or synthetic multivalent glycans with proteins other than lectins, for example with glycosyl hydrolases (glycosidases).[8-11, 13, 15-17,43-46]) Glycosidases constitute a large and important family of enzymes that are responsible for assuring the proper biosynthesis and/or biodegradation of glycoproteins, glycolipids and also proteoglycans - the very entities that serve as ligands for complimentary lectins in *vivo*.

We herein examine the behaviour of glycosidases towards a series of glycan-conjugated nanodiamonds (glyco-ND). Diamond nanoparticles (also termed nanodiamonds) are amongst the most promising new carbon-based materials currently being evaluated for biomedical applications.[18-25] Advantages over related conjugated based on fullerenes and carbon nanotubes include their complete inertness, optical transparency, lack of significant cytotoxicity in a variety of cell types,[26-28] as well as their ease of functionalization through a variety of methods depending on ultimate application. Mannose-functionalized ND, for example, has been shown to inhibit yeast-agglutination as well as human bladder-cell adherence by *E. coli* and most notably to be able to disrupt biofilm formation.[18, 19] Indeed, the usefulness of various ND adducts for the interrogation of glycan-mediated processes has been substantiated recently in a number of reports.[18, 19, 25, 29, 30]

In an extension of this work we were curious to establish that these *O*-glycoside-conjugated ND were indeed stable to the hydrolytic action of glycosidases and report herein the unprecedented finding that monosaccharide substrates of selected glycosyl hydrolases are not only stable to hydrolysis but moreover to behave as competitive, reversible inhibitors of their complementary (matching) glycosidase, simply upon being conjugated in a multivalent fashion to an ND edifice. Also striking is the finding that multivalent presentation of a given monosaccharide motif on an ND can see the "switching on" of the inhibition of non-complementary (mismatching) glycosidases in a surface density-dependent manner.

2. Experimental section

2.1. Materials

N,*N'*-dicyclohexylcarbodiimide (DCC), 4-dimethyl aminopyridine (DMAP), anhydrous acetonitrile, L-ascorbic acid, copper(II) sulphate pentahydrate ($CuSO_4 \cdot 5H_2O$, ≥98%), propargyl alcohol, ethylenediaminetetraacetic acid (EDTA), phenol, sulfuric acid (H_2SO_4), sodium ascorbate (≥98%), L-ascorbic acid, methanol (MeOH), dichloromethane (DCM), acetonitrile, ethanol, *tert*-butanol (tert-BuOH) and sodium methoxide were obtained from Sigma-Aldrich and used without any further purification.

Methyl 4-azidobenzoate solution in *tert*-butyl methyl ether (≥95%) and 4-azidobenzoic acid was purchased from TCI Europe, Belgium.

The glycosidases β-glucosidase (from bovine liver, cytosolic), α-galactosidase (from *Aspergillus niger*), α-galactosidase (from green coffee beans), β-glucosidase (from almonds), amyloglucosidase (from *Aspergillus niger*), α-glucosidase (maltase, from yeast), isomaltase (from yeast), naringinase (*Penicillium decumbens*), β-mannosidase (from *Helix pomatia*) and α-mannosidase (from jack bean) were used in the inhibition studies, as well as the corresponding *o*- and *p*-nitrophenyl glycoside substrates, concanavalin A, horse-radish peroxidase-labelled concanavalin A, yeast mannan and 2,2'-azinobis-(3-ethylbenzothiazoline-6-sulfonic acid) diammonium salt (ABTS) were purchased from Sigma Chemical Co. Milli-Q water (18 MΩ) was used for all experiments. Hydroxylated diamond (ND-OH) particles were obtained from the International Technology Centre, Raleigh, NC, USA. All reagents and solvents were used without further purification unless stated.

2.2. Synthesis of *O*-mannoside (1) and *O*-glucoside (2) (monovalent substrates)

2.2.1 Methyl-4-[4-((α-D-mannopyranosyloxy)methyl)-1*H*-1,2,3-triazol-1-yl]-benzoate (1): Ligand (1) was synthesized according to the literature with some modifications.[3] A mixture of propargyl-mannose (45 mg, 0.21 mmol, 1.0 eq), 0.5 M of methyl 4-azidobenzoate solution in *tert*-butyl methyl ether (619 μL, 0.31 mmol, 1.5 eq), $CuSO_4 \cdot 5H_2O$ (13 mg, 0.05 mmol, 0.25 eq) and sodium ascorbate (18 mg, 0.11 mmol, 0.5 eq) was dissolved in degassed *tert*-BuOH/H_2O (1:1, 8 mL) under nitrogen. After stirring for 1 day at 50 °C, the solvents were removed in vacuum and the crude mixture was purified by silica gel chromatography (DCM/MeOH 9:1) to yield ligand (1) as a colorless solid (48 mg, yield 59%); $[\alpha]_D$ +50.8 (*c* 0.4, MeOH). R_f 0.28 (4:1 DCM-MeOH). ^{1}H NMR (300 MHz, CD_3OD): δ 8.68 (s, 1H, H-9), 8.22 (d, *J* = 8.9 Hz , 2H, Ar*H*), 8.02 (d, *J* = 8.91 Hz , 2H, Ar*H*), 4.92 (d, *J* = 1.4 Hz, 1H, H-1), 4.90 (d, *J* = 12.5 Hz, 1H, H-7b), 4.76 (d, *J* = 12.5 Hz, 1H, H-7a), 3.94 (s, 3H, OCH_3), 3.89 – 3.76 (m, 5H, H-2, H-3, H-4, H-6a, H-6b), 3.61 – 3.59 (m, 1H, H-5) ; ^{13}C NMR (75 MHz, CD_3OD): δ 167.4 (C=O), 146.7 (C8), 141.6, 132.3 (s), 131.0 (Ar), 123.6 (C9), 121.2 (s) (Ar), 101.1 (C1), 75.1 (C5), 72.5 (C3), 72.1 (C2), 68.7 (C4), 63.1 (C6), 60.8 (C7), 52.9 (OCH_3); HRMS (ESI+): calcd.for $C_{17}H_{21}N_3O_8$ $[M + Na]^+$ 418.1221; found 418.1221; HPLC (C4, 254 nm): t_R = 10.065 (93.9%) (Supporting information **Figure S1**).

2.2.2 Methyl 4-[4-((α-D-glucopyranosyloxy)methyl)-1*H*-1,2,3-triazol-1-yl]-benzoate (2): A mixture of propargyl-glucose (35 mg, 0.16 mmol), 0.5 M of methyl 4-azidobenzoate solution in *tert*-butyl methyl ether (482 μL, 0.24 mmol), $CuSO_4 \cdot 5H_2O$ (10 mg, 0.04 mmol) and sodium ascorbate (14 mg, 0.09 mmol, 0.5 eq) was dissolved in degassed *tert*-BuOH/H_2O (1:1, 6 mL) under nitrogen. After stirring for 1 day at 50 °C, the solvents were removed in vacuo and the crude product was purified on silica gel chromatography (DCM/MeOH 9:1) to yield ligand (2) as a colorless solid (49 mg, yield 77%); $[\alpha]_D$ = +56.1 (*c* 0.6, MeOH). R_f 0.44 (4:1 DCM-MeOH). ^{1}H NMR (300 MHz, CD_3OD): δ 8.69 (s, 1H, H-9), 8.22 (d, *J* = 8.9 Hz , 2H, Ar*H*), 8.01 (d, *J* = 8.91 Hz, 2H, Ar*H*), 4.97 (d, *J* = 3.75 Hz, 1H, H-1), 4.93 (d, *J* = 12.7 Hz, 1H, H-7b), 4.78 (d, *J* = 12.7 Hz, 1H, H-7a), 3.94 (s, 3H, OCH_3), 3.85–3.26 (m, 6H, H-2, H-3, H-4, H-6a, H-6b, H-5), ^{13}C NMR (75 MHz, CD_3OD): δ ^{13}C NMR (75 MHz, MeOD) δ 167.3 (C=O), 146.9 (C8), 141.6, 132.3 (s), 131.6 (Ar), 123.5 (C9), 121.2 (s) (Ar), 99.9 (C1), 75.1 (C5), 74.1 (C3), 73.5 (C2), 71.8 (C4), 62.7 (C6), 61.6 (C7), 52.9 (OCH_3); HRMS (ESI+): calcd.for $C_{17}H_{21}N_3O_8$ $[M + Na]^+$ 418.1221; found 418.1220; HPLC (C4, 254 nm): t_R = 9.525 (98.8%)(Supporting information **Figure S1**).

2.3. Modification of diamond nanoparticles

2.3.1. Azide-terminated ND particles (ND-N₃): The functionalization of the ND particles was carried out essentially as described previously for Man-ND:[18] 4-Azidobenzoic acid (0.20 mmol), DCC (0.22 mmol) and DMAP (0.066 mmol) were dissolved in 5 mL anhydrous acetonitrile. A suspension of ND-OH particles (10 mg) in anhydrous acetonitrile (5 mL) was added and the mixture stirred at room temperature for 24 h under nitrogen. The formed ND-N₃ particles were isolated by centrifugation at 10.000 rpm, purified through four consecutive wash/centrifugation cycles at 10.000 rpm with acetonitrile and ethanol, and finally oven dried at 50 °C for 24 h.

2.3.2. Fabrication of Man-, Glc- and Glc/Man-ND (Multivalent Particles): ND-N₃ particles (10 mg) were dispersed in water (10 mL) and sonicated for 30 min. The "click" reaction was performed by addition of an alkynyl carbohydrate (2 mM) followed by $CuSO_4 \cdot 5H_2O$ (200 μM) and L-ascorbic acid (300 μM) and subsequent stirring of the resulting suspension for 24 h at room temperature. The crude sugar-conjugated nanoparticles were isolated by centrifugation at 10.000 rpm. In order to remove residual copper a first cleaning step protocol consisting of three washing/centrifugation cycles with EDTA (1 mM solution in water) was implemented. A second cleaning protocol involving three consecutive washing/centrifugation cycles at 10.000 rpm with a water-ethanol mixture was also carried out. The resulting particles were finally oven-dried at 50 °C for 24 h prior to use.

For the Glc-ND (50 %) and Man-ND (50 %), the appropriate sugar (1 mM) and propargyl alcohol (1 mM) were mixed prior to being subjected to the 'click' reaction with ND-N₃ (10 mg) and processed as described above. Similarly, for the Glc/Man-ND ("mixed"), propargyl glucoside and propargyl mannoside (1 mM) were mixed with ND-N₃ (10 mg) prior to being subjected to "click" conditions and processes as described above.

2.4 Determination of the carbohydrate loading:
A calibration curve was established as previously described.[18] Thus, a phenolic aqueous solution (5 wt%, 60 μL) and concentrated H_2SO_4 (900 μL) was added to an aqueous carbohydrate solution (60 μL), stirred for 10 min and then an absorption spectrum of the mixture was recorded (Perkin Elmer *Lambda 950 dual beam) against a blank sample (without carbohydrate)*. The absorbance of the solution was measured at two wavelengths: λ_1=495 and λ_2=570 nm and the absorbance difference $(A_{495} - A_{570})$ plotted against the concentration of the corresponding carbohydrate. The quantity of surface-linked carbohydrate on glyco-ND was determined with a 60μL aliquot of the corresponding ND particles solution in water, which was treated with phenol/H_2SO_4 following the same protocol described above. Propargyl alcohol-terminated ND particles were subjected to the identical protocol and served as a blank sample.

2.5. Instrumentation

2.5.1. Fourier transform infrared (FTIR) spectroscopy: FTIR spectra were recorded using a Perkin-Elmer Spectrum One FT-IR spectrometer with a resolution of 4 cm⁻¹. Dried ND powder (1 mg) was mixed with KBr powder (100 mg) in an agate mortar. The mixture was pressed into a pellet under 10 tons load for 2-4 min and the spectrum was recorded immediately. Sixteen accumulative scans were collected. The signal from a pure KBr pellet was subtracted as a background.

2.5.2. Particle size measurements: ND suspensions (20 μg.mL⁻¹) in water were sonicated. The particle size of the ND suspensions was measured at 25°C using a Zetasizer Nano ZS (Malvern Instruments S.A., Worcestershire, U.K.) in 173° scattering geometry and the zeta potential was measured using the electrophoretic mode.

2.5.3 NMR data: ¹H NMR spectra were recorded with a Bruker Advance 300 MHz spectrometer using the deuterated solvent as the lock and TMS as an internal standard. Chemical shifts (δ) and coupling constants (*J*) are expressed in ppm and Hertz (Hz), respectively.

2.5.4. Transmission electron microscopy (TEM): TEM measurements were performed on a FEI Tecnai G2-F20 microscope.

2.5.5. X-ray photoelectron spectroscopy (XPS): XPS measurements were performed in a Specs analysis chamber, equipped with a monochromatized Al K_α X-ray source (hν = 1486.74 eV) and a Phoibos 150 mm radius hemispherical electron energy analyzer. The analyzer (constant) pass energy was set to 100 eV for survey spectra and at 20 eV for high resolution scans, with an estimated total (source + analyzer + core hole width) resolution of 0.85 eV for the N 1s spectra. The pressure in the analysis chamber was in 10^{-8} Pa vacuum range, and an electron flood gun operating at 1 eV energy and 100 μA electron current was used to ensure sample neutralization. Electrons are recorded at normal emission in "Large Area Mode" of the Phoibos analyzer. The XPS data presented have been deconvoluted using mixed Lorentz/Gauss profiles and the CasaXPS software.

2.5.6. GC-FID analysis: GC-FID was carried out using an Agilent 7820A chromatograph with an EPC injector fitted with a cross-linked 5% phenyl-dimethylsiloxane column (HP-5; 30 m x 320 μm x 0.25 μm). Operating conditions were: injection port temperature 310 ºC; splitting ratio 25:1; injection volume 1 μL of derivatized samples; column oven temperature programmed from180 to 310 ºC at 5 ºC min⁻¹, with a 25 min hold at 310 ºC; carrier gas helium (constant flow at 1.2 mL min-1); detector port temperature 310 ºC. Total acquisition time was 45 min. The identity of D-mannose (elution time 4.8/5.1 min) and D-glucose (elution time 4.9/5.2) was confirmed by comparison with the GC chromatograms of authentic samples. Calibration curves for quantitative determination were built by using a range of concentrations, from which response factors relative to the I.S. (elution time 8.3/8.5 min) were determined.

2.6. Bioassays

2.6.1. Inhibition assay to determine the interactions of Man-ND, Glc-ND, Man-ND (50 %), Glc-ND (50 %) and Glc/Man-ND with glycosidases: Inhibitory potencies were determined by spectrophotometrically measuring the residual hydrolytic activities of the glycosidases against the respective *o*- (for β-glucosidase/β-galactosidase from bovine liver) or *p*-nitrophenyl α- or β-D-glycopyranoside, in the presence of the corresponding iminosugar derivative. Each assay was performed in phosphate or phosphate-citrate (for α- or β-mannosidase or amyloglucosidase) buffer at the optimal pH for each enzyme. The K_m values for the different glycosidases used in the tests and the corresponding working pH are listed herein: β-glucosidase (bovine liver), K_m = 2.0 mM (pH 7.3); α-glucosidase (yeast), K_m = 0.35 mM (pH 6.8); β-glucosidase (almonds), K_m = 3.5 mM (pH 7.3); α-galactosidase (coffee beans), K_m = 2.0 mM (pH 6.8); amyloglucosidase (*Aspergillus niger*), K_m = 3.0 mM (pH 5.5); naringinase (*Penicillium decumbes*), K_m = 2.7 mM (pH 6.8); β-mannosidase (*Helix pomatia*), K_m = 0.6 mM (pH 5.5); α-mannosidase (jack bean), K_m = 2.0 mM (pH 5.5). The reactions were initiated by addition of enzyme to a solution of the substrate in the absence or presence of various concentrations of inhibitor. After the mixture

was incubated for 10-30 min at 37 ºC the reaction was quenched by addition of 1 M Na$_2$CO$_3$. The absorbance of the resulting mixture was determined at 405 nm or 505 nm. The K_i value and enzyme inhibition mode were determined from the slope of Lineweaver-Burk plots and double reciprocal analyses using a Microsoft Office Excel 2003 program.

2.6.2. Procedures to monitor the stability of glyco-ND and the monovalent reference ligands (1 and 2) towards α-mannosidase and α-glucosidase: The susceptibility of glyco-ND and the monovalent α-D-mannopyranosyl and α-D-glucopyranosyl glycosides (**1**) and (**2**) towards α-mannosidase and α-glucosidase hydrolysis was examined by incubating each conjugate with the corresponding enzyme at 37 ºC under identical conditions to those above described for determination of the inhibition constants during 1 h and monitoring the formation of free mannose or glucose by gas chromatography (GC). For GC analysis, the samples were subjected to an oximation-trimethylsilylation protocol as reported in Ref.[31] Briefly, immediately after quenching, the samples were freeze-dried. To 15-20 mg of each sample, de-ionized water (1 mL) was added. To 100 μL of the resulting solution was then added 100 μL of internal standard (I.S.; 4 mg mL^{-1} phenyl β-D-glucopyranoside in acetone-water 1:9, v/v) and the final solution was evaporated to dryness at 60 ºC (drying oven). The residue was treated with 1 mL of a solution of hydroxylamine in pyridine (20 mg mL^{-1}) at 60 ºC over 50 min. with mixing at intervals. Hexamethyldisilazane (200 μL) and trimethylchlorosilane (100 μL) were then added, and the reaction mixtures were kept at 60 ºC over a further 40 min period. Formation of a white precipitate was observed during this operation, which was separated by centrifugation (13.000 rpm, 5 min) before injection in the GC apparatus. It is worth noting that following oximation-trimethylsilylation derivatization, reducing monosaccharides, provide two peaks in the GC chromatograms, corresponding to the syn- and anti-TMS-oximes, whereas the I.S. provides a single peak.

2.6.3. Enzyme-Linked Lectin Assay (ELLA): Nunc-Inmuno™ plates (MaxiSorp™) were coated overnight with yeast (*Saccaromices cerevisae*) mannan at 100 μL/well diluted from a stock solution of 10 μg·mL^{-1} in 0.01 M phosphate buffer saline (PBS, pH 7.3 containing 0.1 mM Ca^{2+} and 0.1 mM Mn^{2+}) at room temperature. The wells were then washed three times with 300 μL of washing buffer (containing 0.05% (v/v) Tween 20) (PBST). The washing procedure was repeated after each of the incubations throughout the assay. The wells were then blocked with 150 μL/well of 1% BSA/PBS for 1 h at 37 ºC. After washing, the wells were filled with 100 μL of serial dilutions of horseradish peroxidase-labelled concanavalin A lectin (ConA-HRP) from 10^{-1} to 10^{-5} mg mL^{-1} in PBS, and incubated at 37 ºC for 1 h. The plates were washed and 50 μL/well of 2,2'-azinobis-(3-ethylbenzothiazoline-6-sulfonic acid) diammonium salt (ABTS) (0.25 mg·mL^{-1}) in citrate buffer (0.2 M, pH 4.0 with 0.015% H$_2$O$_2$) was added. The reaction was stopped after 20 min by adding 50 μL/well of 1 M H$_2$SO$_4$ and the absorbances were measured at 405 nm. Blank wells contained citrate-phosphate buffer. The concentration of lectin-enzyme conjugate that displayed an absorbance between 0.8 and 1.0 was used for inhibition experiments.

In order to carry out the inhibition experiments, each glyco-ND or the control non-glycosylated ND sample was added in a serial of 2-fold dilutions (60 μL/well) in PBS with 60 μL of the desired ConA-peroxidase conjugate concentration on Nunclon™ (Delta) microtiter plates and incubated for 1 h at 37 ºC. The maximum concentration was kept in all cases at 150 μM to prevent aggregation phenomena; below this concentration, no precipitation was observed under the experimental setup. The

above solutions (100 μL) were then transferred to the mannan-coated microplates, which were incubated for 1 h at 37 ºC. The plates were washed and the ABTS substrate was added (50 μL/well). Color development was stopped after 20 min and the absorbances were measured. IC$_{50}$ values, assumed to be proportional to the corresponding binding affinities, were calculated from the percentages of inhibition with up to eleven different concentrations of each conjugate sample as follows:

% Inhibition = ($A_{\text{(no inhibitor)}}$ - $A_{\text{(with inhibitor)}}$)/$A_{\text{(no inhibitor)}}$ x 100

Results in triplicate were used for the plotting the inhibition curves for each individual ELLA experiment. Typically, the IC$_{50}$ values (concentration required for 50% inhibition of the Con A-yeast mannan association) obtained from several independently performed tests were in the range of ±12%. Nevertheless, the relative inhibition values calculated from independent series of data were highly reproducible.

2.6.4. Two-site ELLA (sandwich assay): Nunc-Inmuno™ plates (MaxiSorp™) microtitration plates were coated with yeast mannan and blocked with BSA as described above. Unlabelled (therefore cross-linkable) ConA lectin was then added at 100 μL/well from a stock solution of 5 μg/mL in 0.01 M phosphate buffer (PBS, pH 7.3, containing 0.1 mM Ca^{2+} and 0.1 mM Mn^{2+}) for 2 h at 37 °C. The synthesized glyco-ND and the hydroxylated-ND negative control were used as stock solutions of 0.15 mmol/mL in PBS. The ligands were added in serial 2- to 10-fold dilutions (50 μL/well) in PBS and incubated at 37 °C. After 1 h, horseradish peroxidase-labeled ConA lectin (50 μL/well of 200-fold dilution of a 1 mg/mL stock solution in PBS, pH 7.3, containing 0.1 mM Ca^{2+} and 0.1 mM Mn^{2+}) was added to the microtiter plates which were incubated for another hour at 37 °C. The plates were washed with PBS, and 50 μL/well of ABTS (1 mg/4 mL) in citrate-phosphate buffer (0.2 M, pH 4.0 with 0.015% H$_2$O$_2$) was added. The reactions were stopped after 30 min by adding 50 mL/well of 1 M H$_2$SO$_4$, and the optical density was measured at 405 nm relative to 570 nm (**SI Figure S4**).

2.6.5. Turbidity Assay: Solutions of the glyco-ND (50 μL) at the appropriate concentration (37.5, 18.7 and 9.3 μM) in PBS were added to a solution of ConA (50 μL; 1 mg mL^{-1} in PBS, pH 7.3, containing 0.1 mm Ca^{2+} and 0.1 mm Mn^{2+}). The time-dependent turbidity kinetics was recorded by measuring the absorption coefficient at 490 nm at intervals of 1 min for 35 min. After 15 min, D-mannose was added to the suspensions to have an excess of about 2500-, 5000- and 10.000-fold relative to the ND sugar content to check the reversibility of the aggregation (**SI, Figure S5, A-C**). The initial rate of precipitation (V_i) was determined by linear fits of the initial portion of the data (**SI, Figure S5, D**).

2.6.6. Two-Site Competitive Lectin—Glycosidase Enzyme-Linked Lectin Assay: Nunc-Inmuno™ plates (MaxiSorp™) microtitration plates were coated with yeast mannan, blocked with BSA as described above and further coated with unlabelled ConA lectin at 100 μL/well of a stock solution of 5 μg/mL in 0.01 M phosphate buffer (PBS, pH 7.3, containing 0.1 mM Ca^{2+} and 0.1 mM Mn^{2+}) for 2 h at 37 °C. The glyco-ND, used as 75 μM solutions in PBS, were then added (50 μL/well) and incubated at 37 °C. At this concentration, a classical two-site ELLA (see above) provided optical density values in the range 0.61 to 0.45 (A.U.), which were normalized at 100% cross-linking for the lectin-glycosidase competition experiments. The, yeast maltase in serial 2-fold dilutions (50 μL/well) from a stock solution of 40 U/mL in PBS and ConA-HRP lectin (50 μL/well of 100-fold dilution of a 1 mg/mL stock solution in PBS) were added and the microtitre plates were incubated at 37 °C. The plates were washed with PBS and 50 μL/well of 2,2'-azinobis-(3-
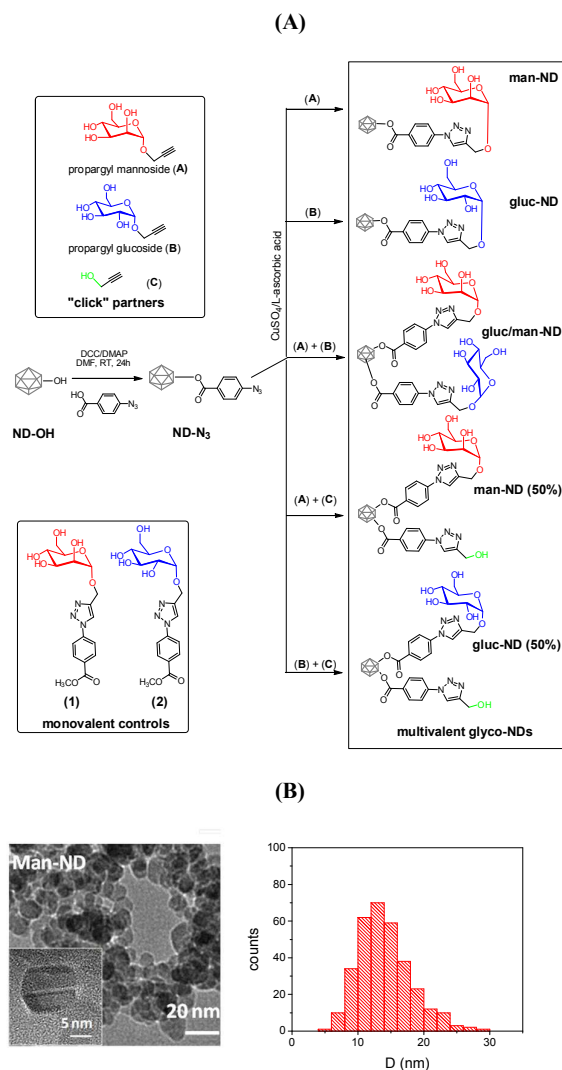
ethylbenzothiazoline-6-sulfonic acid) diammonium salt (ABTS, 1 mg/4 mL) in citrate-phosphate buffer (0.2 M, pH 4.0 with 0.015% H_2O_2) was added. The reactions were stopped after 30 min by adding 50 μL/well of 1 M H_2SO_4. The optical density was then measured at 410 nm relative to 570 nm and plot against maltase concentration (**SI Figure S6**). Control experiments were conducted to confirm that the enzyme itself did not interact with ConA and that it retained its catalytic activity under the conditions of the assay.

3. Results and Discussion

The behavior of α-mannosidase from jack bean and α-glucosidase from yeast, towards the corresponding α-mannosides and α-glucosides, respectively, when free in solution or upon being grafted on ND, was selected as the primary focus of the present investigation. The latter enzymes are commercially available and are routinely used for ascertaining the potency and selectivity patterns of putative glycosidase inhibitors. Moreover, simple α-mannosides and α-glucosides are accepted as substrates by their respective α-mannosidase and α-glucosidase (matching enzymes). For the sake of completeness, a β-mannosidase, a β-glucosidase and also α- and β-galactosidases, none of which act on either α-mannosides or α-glucosides, were included in the evaluation panel (mismatching enzymes). α-*O*-Mannoside- and α-*O*-glucoside-grafted-ND (Man- and Glc-ND, respectively) as well as particles featuring 50% of the maximal surface loading of either sugar (Man-ND (50%) and Glc-ND (50%)) were targeted for evaluation (**Figure 1**). In addition, a mixed glyco-ND comprising equal proportions of both α-D-mannopyranoside and α-D-glucopyranoside moieties conjugated on their surface was also fabricated (Glc/Man-ND) for study.

3.1. Preparation and characterisation of ND-conjugates and *O*-glycoside monomers

The strategy for the preparation of all sugar-conjugated ND studied herein involved the "click" reaction between azide-terminated particles (ND-N_3) and the appropriate propargylated partner(s) in the presence of CuSO$_4$/L-ascorbic acid as catalyst, as previously described (**Figure 1A**).[18] The successful integration of glycans onto the ND surface was confirmed by XPS and FTIR analysis (**Supporting Information, Figure S2A, B**).

Figure 1. (A) Strategy for fabrication of glyco-ND as well as the structures of monomers and ND-conjugates evaluated in this work; (B) TEM image of Man-ND together with the corresponding size distribution. See text for details.

A representative transmission electron microscopy (TEM) image of Man-ND (**Figure 1B**) reveals the presence of spherical particles with a mean diameter of 12 ± 4 nm. The data was obtained from an analysis of several hundreds of NPs. The surface-modified layer is not visible in the TEM due to its high transparency to the electron beam. The calculated hydrodynamic diameter of glycan-modified ND is a composite value as they partially aggregate in solution (**Table 1**). The value however remains unchanged over days, indicating that the conjugates have good colloidal stability in aqueous media. For a complete set of TEMs at each stage of NP functionalization, see **Supporting Information, Figure S2C**. The complete characterisation data and physico-chemical properties, including the particle diameter and zeta potential of all fabricated particles are summarized in **Table 1**. The total amount of sugar conjugated to a given particle was quantified using the classical phenol-sulphuric acid method. The analysis confirmed that the 50% loaded particles contained half the quantity of sugar present on the 100% loaded NPs (**Table 1**). It has to be noted that the phenol/sulfuric acid method does not allow discrimination between manno and glycopyranosides, but we make the reasonable approximation that the mixed ND comprise equal portions of Glc/Man on the surface. The corresponding monovalent α-*O*-mannoside and α-

O-glucoside control conjugates (**1**) and (**2**) (**Figure 1A**) required for the study were synthesised by the Cu(I)-catalysed "click" reaction of the appropriate propargyl α-glycoside with 4-azidobenzoic acid methyl ester and proceeds smoothly.

ND scaffold	Hydrodynamic diameter (nm)	Zeta potential (mV)	Sugar loading (µg mg⁻¹ ND)	Sugar loading (glycans /ND)
ND-OH	79 ± 13	35.3 ± 1.6	-	-
Man-ND	155 ± 4	26.7 ± 0.6	96 ± 7	(43±16) ×10³
Glc-ND	145 ± 3	24.7 ± 0.2	113 ± 5	(50±21) ×10³
Glc/Man-ND	124 ± 12	27.0 ± 0.2	110 ± 5	(49±20) ×10³
Man-ND (50 %)	101 ± 10	28.0 ± 0.6	50 ± 3	(22±13) ×10³
Glc-ND (50 %)	92 ± 2	28.1 ± 0.8	55 ± 3	(25±11) ×10³

Tab1e 1. Summary of selected physico-chemical properties of ND-OH and ND-conjugates. See text for details.

3.2. Subjection of *O*-glycoside—ND conjugates and monomers to the hydrolytic action of glycosidases

As expected the monovalent analogs (**1**) and (**2**) are hydrolysed by their appropriate partner enzymes, namely α-mannosidase or α-glucosidase, respectively, but remain inert to the hydrolytic action of all other glycosidases tested (gas chromatography monitoring, see supporting information **Figure S3**).

Having established the hydrolytic susceptibility of these *O*-glycoside monomers free in solution, their behaviour upon being presented multivalently on the ND surface was examined against the same panel of enzymes. In order to ascertain how the glyco-ND are recognised by ConA they were subjected to an enzyme-linked lectin assay (ELLA). This reports on the ability of a soluble saccharide to inhibit the association between a labelled lectin (here ConA lectin labelled with horseradish peroxidase, ConA-HRP) and a ligand immobilized on the microtiter well (here a yeast mannan). Conjugation of ConA to the HRP protein label (40 kD) precludes the possibility that two conjugates might interact with one another, and thus assures that only 1:1 binding stoichiometries occur with the saccharide ligand. In order to discount that the ND scaffold itself might have a bearing on the outcome of the assay, a conjugate featuring exclusively hydroxymethyltriazolyl chains (devoid of any glycotope) was included as a negative control. Methyl α-D-mannopyranoside and methyl α-D-glucopyranoside were also included as monovalent positive controls.

Remarkably, both Glc-ND and Glc-ND (50%), when treated with the α-glucosidase from baker's yeast under classical assay conditions, revealed themselves to be completely stable to hydrolysis (the formation of mannose was not detectable by gas chromatography even upon incubation under assay conditions for 24 h at 37 ºC; **Figure S3**) and instead behaved as competitive inhibitors of the enzyme, with inhibition constant (K_i) values of 22 and 5.5 µM, respectively. The required hydroxyl-coated ND-conjugate (**ND-OH**) negative control was prepared by clicking propargyl alcohol and 4-azidobenzoate-modified ND particles (precursors **C** and **ND-N₃** in **Figure 1A**). Although the low water solubility of **ND-OH** prevented an exhaustive evaluation, no significant glycosidase inhibition was observed at low mM concentrations, suggesting that the ND scaffold itself did not contribute significantly to the observed inhibitory activity. The Glc/Man-ND also displayed a similarly low K_i value of 1.9 µM (**Table 2**). Screening inhibitory activities of Glc-ND against the amyloglucosidase (1,4-α-D-glucan glucohydrolase) from *Asp.*

Niger and the isomaltase (oligosaccharide α-1,6-glucohydrolase) from baker's yeast, both of which hydrolyse α-glucosidic substrates, established none to be inhibitors of the former enzyme but all to inhibit the activity of the latter with K_i's of 14.0, 4.3 and 5.5 µM (for Glc-ND, Glc-ND (50%) and Glc/Man-NDs, respectively). In a parallel series of experiments, Man-ND, Man-ND (50%) and Glc/Man-ND were screened against α-mannosidase from jack bean. These conjugates are seen to be comparatively poor inhibitors of their target enzyme giving respectively, K_i's of 517, 295 and 407 µM. Again, as expected the corresponding monomeric *O*-mannoside (**1**) behaves as a substrate for the jack bean α-mannosidase being efficiently hydrolysed under standard assay conditions, whereas under the same conditions the corresponding *O*-mannoside-conjugated ND remains intact.

Although the origin of the inhibitory behaviour of the glyco-ND particles remains to be established, the finding that they do act as such is nonetheless unprecedented. Exposure of glycosidases to a fixed concentration of a glyco-ND for prolonged periods (up to 2 h), far in excess of the assay time, saw no observable change in catalytic activity, discounting any possibility that protein denaturation by the glyco-NDs contributed to the observed inhibitory effects. The levels of inhibition observed for these ND-grafted *O*-glycosides are better appreciated if compared with K_i values displayed by 1-deoxynojirimycin (DNJ), the archetypical natural glucosidase inhibitor.[15-17] DNJ, under identical assay conditions to those used to screen the sugar-grafted ND particles, inhibits baker's yeast α-glucosidase with a K_i of 25 µM, an order of magnitude higher than the mixed-ND (K_i 1.9 µM). In addition, the glyco-ND particles are seen indeed to exhibit some degree of selectivity, behaving as better inhibitors of certain enzymes than others, with a pattern of selectivity that does not always parallel that observed for DNJ (**Table 1**). Baker's yeast isomaltase is inhibited for example by Glc-ND (50%) with a K_i of 4.3 µM and also by DNJ (K_i of 11 µM). In contrast the amyloglucosidase from *Asp. Niger* is strongly inhibited by DNJ (K_i of 2.1 µM), whereas none of the sugar-grafted particles had any effect on this particular activity.

In a bid to better understand the inhibitory activity observed for the various *O*-glycoside-conjugated ND particles, they were subjected to further scrutiny as inhibitors of various mismatching enzymes (those that do not accept either α-*O*-glucosides or α-*O*-mannosides as substrates). Thus, the Glc-ND (featuring α-configured *O*-glucosidic units) when screened against the β-glucosidase from bovine liver, was observed to be inhibitory with K_i values of 113 and 44 µM for the Glc-ND and the Glc-ND (50%), respectively and a K_i of 192 µM for the Glc/Man-ND. The Glc-ND proved a poorer inhibitor of a second β-glucosidase (from almond), giving K_i's of 359, 169 and 784 µM for the corresponding 100%, 50% and mixed-sugar conjugates, respectively. Further, although neither the Glc-ND or Man-ND show activity as inhibitors of the β-mannosidase from *Helix pomatia*, at the maximum concentrations tested, the Glc-ND (50%), Man-ND (50 %) and also the mixed-ND particles unexpectedly did, with K_i's of 55, 75 and 74 µM, respectively (**Table 2**). The absence of inhibition by the 100%-loaded ND is difficult to explain with certainty at present but might simply be due to the relative inaccessibility of the ligand to this particular β-mannosidase at the highest carbohydrate surface loadings.
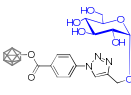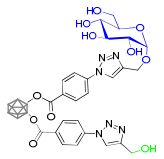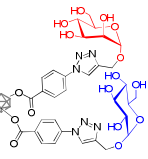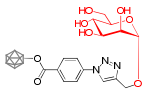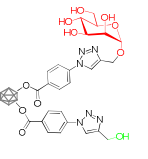
We were intrigued by the relatively relaxed inhibitory specificity shown by the Glc-ND and were curious to establish whether this was limited solely to glycosidases acting on α-D-*gluco*- or α-D-*manno*-configured substrates. The Glc-ND were thus tested against two additional activities: the α-galactosidase from green coffee bean and the β-galactosidase from *E. coli*. Both the Glc-

ND and the Glc-ND (50%) were found to inhibit the α- and β-galactosidases with almost identical potency (K_i's in the range 13-33 μM; **Table 2**). The Glc/Man-ND inhibited both galactosidase activities but differentially, giving a K_i of 69 μM for the α-galactosidase and a value of 268 μM for the β-enzyme (**Table 2**).
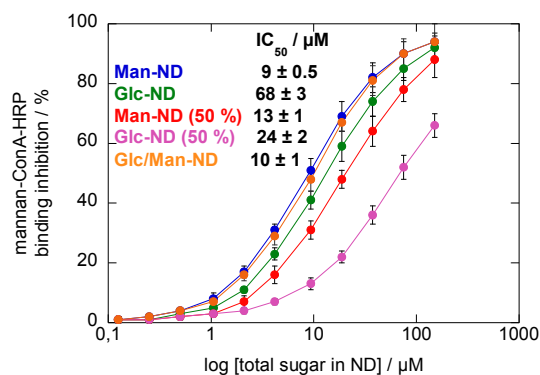
That *O*-glycoside configurational complementarity is not an absolute prerequisite for effective enzyme inhibition by Glc-ND is particularly well borne out by their pronounced inhibition of mismatching glycosidases. This latter observation prompted us to examine the effects of the *O*-mannoside-grafted ND on the complete panel of activities at our disposal, even though these latter conjugates were seen to exhibit only negligible inhibition

of the "matching" mannosidase activity. The screening reveals that both the Man-ND and the Man-ND (50%) inhibit the baker's yeast α-glucosidase activity and very significantly so, with K_i's of 9.4 and 1.3 μM, respectively (**Table 2**). The β-glucosidase from bovine liver is however more poorly inhibited compared to the α-enzyme, giving K_i's of 223 and 108 μM for the Man-ND and the Man-ND (50 %), respectively. In addition, the α- and β-galactosidases from coffee bean and *E. coli* respectively, are also strongly inhibited by the Man-ND, with K_i's of 33 and 13 μM for the Man-ND and 21 and 13 μM for Man-ND (50%), respectively, and to an equivalent extent as that observed for the corresponding Glc-ND (**Table 2**).

Table 2. Inhibition constants (K_i, μM) for various glyco-ND, against selected commercial glycosidases.[a] See text for details.

Enzyme	Glc-ND	Glc-ND (50%)	Glc/Man-ND	Man-ND	Man-ND (50%)
α-glucosidase (baker's yeast)	22 ± 2	5.5 ± 0.2	1.9 ± 0.1	9.4 ± 0.3	1.3 ± 0.1
Amyloglucosidase (*Asp. niger*)	NI[b]	NI	NI	NI	NI
Isomaltase (baker's yeast)	14 ± 0.5	4.3 ± 0.2	5.5 ± 0.2	12.0 ± 0.5	2.6 ± 0.2
α-mannosidase (jack bean)	419 ± 35	222 ± 15	407 ± 30	517 ± 50	295 ± 20
β-glucosidase (bovine liver)	113 ± 5	44 ± 2	192 ± 5	223 ± 10	108 ± 5
β-glucosidase (almonds)	359 ± 20	169 ± 10	784 ± 50	323 ± 15	105 ± 5
β-mannosidase (*Helix pomatia*)	NI	55 ± 3	74 ± 5	NI	75 ± 4
α-galactosidase (coffee beans)	31 ± 2	22 ± 2	69 ± 5	33 ± 2	21 ± 2
β-galactosidase (*E. coli*)	22 ± 1	17± 1	268 ± 25	13 ± 2	13 ± 1

[a] Inhibition was reversible and competitive in all cases except for Glc-ND (50%) against yeast α-glucosidase (yeast maltase), for which a mixed-mode inhibition mode was observed. [b] NI: no inhibition observed at 1 mM.

	IC$_{50}$ / μM
Man-ND	9 ± 0.5
Glc-ND	68 ± 3
Man-ND (50 %)	13 ± 1
Glc-ND (50 %)	24 ± 2
Glc/Man-ND	10 ± 1

Figure 2. ELLA plots (logarithm scale) for the inhibition of ConA-HRP binding to yeast mannan with increasing concentrations of the various glyco-ND on a sugar content basis. The corresponding IC$_{50}$ values are expressed as mean ± SD (n = 3). See text for details.

It is worthwhile noting that, while the K_i values recorded for glycoside-coated ND do not vary dramatically from one another with sugar loading (100% *vs* 50%) for the majority of enzymes tested, this trend is seen not to be true for the β-mannosidase from *Helix pomatia*: for the latter enzyme, the 50% Glc- and 50% Man-NDs as well as the mixed ND are inhibitory, whereas the 100% Glc- and Man-ND are not.

The inhibition data suggests that the mode-of-recognition of the *O*-glycoside-grafted particles by a particular glycosidase is quite different from that usually harnessed by that enzyme for monovalent substrate hydrolysis. Non-specific aggregation of the glyco-ND with the tested glycosidases seems improbable considering the observed inhibition activity profiles. Indeed, monosaccharides are currently used as passivation molecules to suppress unspecific interactions of nanoparticles with biomolecules in physiological media.[36, 37] The impact on factors such as glycotope density and heteromultivalency on glycosidase inhibition is more reminiscent of that encountered in carbohydrate-lectin recognition events.[37] We were in a position to establish whether or not this was indeed the case and set about evaluating the performance of the various glyco-ND as ligands
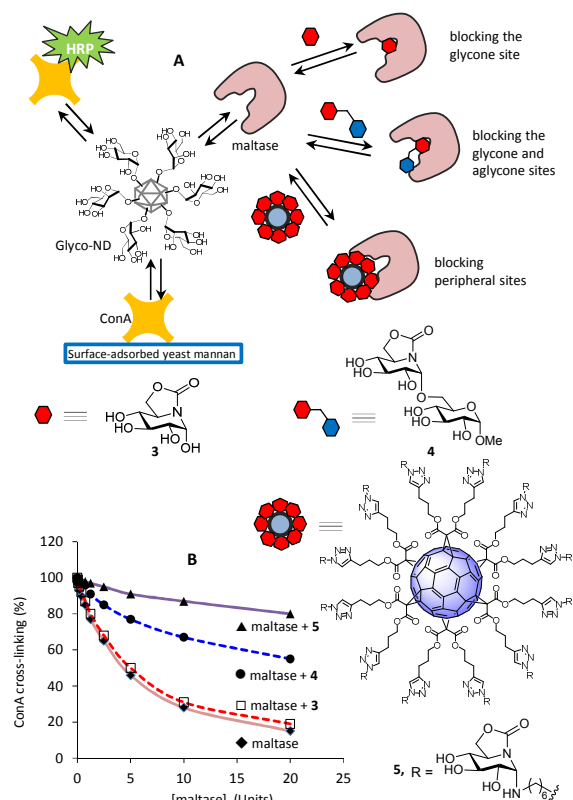
for the lectin concanavalin A (ConA), a tetravalent protein known to recognize both α-D-O-mannopyranosides and α-D-O-glucopyranosides. The abilities of the glyco-ND to bind, cross-link and aggregate ConA as assessed by a range of methods including an enzyme-linked lectin assay (ELLA; **Figure 2**), a two-site sandwich ELLA and a turbidimetry assay, respectively (see supporting information **Figure S4** and **Figure S5**),[36] were duly investigated and indeed seen to reflect their expected *per glycotope* affinity enhancements as compared to monovalent controls: the high avidity of the lectin for each respective glycosylated ND particle is consistent with the manifestation of potent multivalent effects driving lectin recognition and binding.

Sandwich-type competitive glycosidase-lectin ELLA

Having established that Glc- and Man-ND behave as both inhibitors of various glycosidases and as ligands of ConA, a newly developed sandwich-type competitive glycosidase-lectin ELLA was implemented in the hope of garnering further insights into the mechanism(s) of enzyme inhibition by the glyco-ND. The experimental setting is an interface composed of a mannan polysaccharide adsorbed on a polystyrene microtiter well, onto which is applied a second layer constituted of the tetrameric, and therefore cross-linkable, lectin ConA (**Figure 3A**).

We reasoned that, if a glycosidase capable of competing with horseradish peroxidase (HRP)-labelled ConA (HRP-ConA) for binding a given glyco-ND were to be included in the mix, a concentration-dependent decrease in lectin cross-linking would ensue. Moreover, inclusion of an excess of a potent active site-directed inhibitor of the particular glycosidase being tested would furnish an assay that reported *indirectly*, on the extent to which the active site is implicated in any glyco-ND—enzyme complex. We reasoned too that were the assay to be performed with an inhibitor capable of spanning both the catalytic and aglycone binding sites simultaneously, it would then afford insights into the impact of glyco-ND—aglycone binding on inhibition. Yet another variant of this assay, in which advantage would be taken of a fullerene-based inhibitor featuring multiple copies of the same iminosugar glycomimetic motif, was expected to report on the consequences on catalysis of interactions of glyco-ND with peripheral regions of the enzyme (**Figure 3A**).[34] We hoped that the data taken together, would allow the relative individual contributions of either the active site or any peripheral binding region on a particular enzyme, in glyco-ND recognition to be ascertained and thus provide insights into the possible mode(s)-of-inhibition in play.

Figure 3. A) Schematic representation of the ConA—yeast α-glucosidase (maltase) competitive ELLA; the structures of the active site-directed glycone-type inhibitor (**3**) the pseudodisaccharide derivative (**4**) and the multivalent conjugate (**5**), used as controls to map the implication of, respectively, the glycone site, the aglycone site and peripheral sites in glyco-ND binding to the enzyme are depicted. B) Plots of the relative ConA cross-linking capability of Man-ND as a function of maltase concentration in the absence or in the presence of an excess of (**3**), (**4**) or (**5**), respectively (**Figure S6**). See text for details.

The ConA—Glc-ND—HRP-ConA cross-linking inhibition plots for yeast α-glucosidase (yeast maltase) alone or in the presence of the competitive maltase inhibitors nojirimycin 5N,6O-(cyclic carbamate) (**3**) (K_i = 2.2 μM)[34, 38] and methyl 6-O-[nojirimycin-1-yl 5N,6O-(cyclic carbamate)]-α-D-glycopyranoside (**4**) (K_i = 5.5 μM)[39] are each depicted in **Figure 3B**. Both (**3**) and (**4**) are active-site directed inhibitors: compound (**3**), a monosaccharide mimic, binds exclusively at the glycone (-1) site of the enzyme whereas the isomaltose mimic (**4**) spans simultaneously both glycone (-1) and the aglycone (+1) sites. The corresponding plot for the dodecavalent fullerene C[60]-conjugate (**5**)[34] (K_i = 18 μM), generated under identical experimental conditions is also depicted in **Figure 3B**. The fullerene conjugate (**5**) has been demonstrated to adopt a catalytic site-independent binding mode with this same maltase. In the presence of the monosaccharide-like inhibitor (**3**), and thus when the glycone site of maltase is occupied, the data indicates that the ability of the enzyme to compete with the lectin for the Glc-ND is only nominally compromised. In contrast, any ability of the glyco-ND to form an ND-maltase complex is seen to be severely perturbed in the presence of either the pseudodisaccharide homologue (**4**) or the multivalent conjugate (**5**), and consequently, lectin cross-linking is largely unimpeded by either. Identical trends were recorded for the 50% Glc-, 100% and 50% Man-, and mixed Glc/Man-ND conjugates in this assay (see **Figure S6**).

Although the remarkable difference between monovalent and multivalent *O*-glycosides towards the hydrolytic action of

glycosidases revealed herein would appear difficult to reconcile with the typical modes-of-action currently accepted for glycosidases, the evidence of the sandwich type competitive enzyme-lectin ELLA allows a plausible alternative mode-of-inhibition to be put forward for the glyco-ND: one that does not parallel the mode of substrate recognition typical of enzymatic hydrolysis, but that instead implicates the interaction of *O*-glycoside moieties present in glyco-ND with the aglycone binding sites of the target enzymes as one of the primary driving forces underpinning their inhibitory activity. This hypothesis is consistent with the fact that the interaction of a given substrate with the catalytic cleft of a particular enzyme is dependent on the interactions of both its glycone *and* aglycone constituents. Aglycone-binding sites of glycosidases are known to accept a range of structural motifs, and substrates featuring certain of these motifs have been shown be much more susceptible to enzymatic hydrolysis. Indeed, the exploitation of such aglycone site-interactions in glycosidase inhibitor design was recognized some twenty years ago.[40] Glycosidase inhibitors targeting exclusively the aglycone binding site of glucosidases have been reported but are rare.[41] On the other hand, hybrid compounds in which a judiciously selected aglycone moiety and a glycomimetic inhibitor are combined in the same molecule, have been reported to display improved inhibitory potencies and selectivities for their target enzymes compared with compounds featuring only one of the constituent fragments.[42]

As far as we are aware, prior to the present work there has been no report of the transformation of an *O*-glycoside *substrate* of a glycosidase into an *inhibitor*, simply upon being presented multivalently on a scaffold. The resistance of a number of *O*-glycosyl-supported gold NPs to the hydrolytic action of various glycosyl hydrolases has on the other hand been examined previously, although none were reported to be inhibitors of the enzymes tested.[35, 43-45] Although, the recognition of certain carbohydrate-based ligands by lectins and enzymes has on occasion been observed to change dramatically upon being presented multivalently[32-35], we are only aware of a single previous study that explored multivalent *O*-glycosides as glycosidase inhibitors. In that, the large bacterial sialidase from *V. cholerae*, that features a catalytic module flanked by two lectin domains (carbohydrate binding modules or CBMs) was reported to be strongly inhibited by a synthetic polymer featuring multiple *O*-galactosyl units.[46] The latter glycopolymer was proposed to owe its activity to its interaction with the CBMs of the *V. cholerae* sialidase, effectively leading to their "sequestration", resulting in seriously compromising its ability to hydrolyse multivalent *O*-sialoside substrates. The role of CBMs in catalysis has now been widely examined [47-49] but as far as we are aware, catalysis by the enzymes explored in the present study does not benefit from the presence of discrete flanking CBMs. However, binding of multivalent glyco-ND to distal non-catalytic domains other than CBMs of glycosidases would be expected also to lead to a reduction in their catalytic efficiency.[50-52] No such domains have been established for any of the enzymes studied here. Additionally, although the β-galactosidase from *E. coli* features multiple catalytic domains[53] and is thus expected to be susceptible to inhibition by appropriate multivalent constructs - it is nevertheless inhibited by both Glc-ND and the Glc-ND (50%) to the same extent and moreover, only to the same level as seen for the α-galactosidase from coffee bean, which only features a single such domain.

multivalently on the surface of ND particles are not only rendered stable towards the hydrolytic action of the corresponding matching glycosidases, but are also endowed with the ability to competitively and reversibly inhibit these enzymes. Moreover, conjugation of the *O*-glycosides to ND sees them behaving as inhibitors of enzymes for which they do not serve as substrates *even* when in their monovalent, free form. Furthermore, the inhibitory potency of a particular glyco-ND edifice towards a given enzymatic activity is demonstrated to be dependent not only on the particular sugar motif grafted (α-D-*gluco* or α-D-*manno*) but also on whether the glycosidic moieties are presented in homogeneous displays, or as a mixture of glycotopes on a single particle, and moreover to vary with their surface density (100 or 50% loading). The data support that inhibition by the glyco-ND cannot be one that is catalytic site-independent as has previously been put forward to rationalize the mode-of-inhibition of iminosugar constructs.[34] Instead, the data of the ConA—yeast α-glucosidase competitive ELLA support an alternative mode-of-inhibition in which glyco-ND are able to *competitively* inhibit catalytic activity through formation of the corresponding glyco-ND—enzyme complexes by harnessing of interactions with the enzyme aglycone binding sites. That additional modes-of-binding might also be operational for one or more enzymes in the panel tested here, cannot be discounted at this stage and remain to be fully elaborated. However, the distinct preferences for sugar motif recognition, dependence on multivalency, heteromultivalency and architectural parameters of a particular glyco-ND, do parallel closely those previously observed for interactions of multivalent ligands with lectins. The mode-of-inhibition implicating aglycone binding proposed here would support that the modes-of-interaction of glyco-ND with both enzymes and lectins share much in common and begs the question as to whether or not this might also hold true for alternate multivalent carbohydrate analogs.

To the best of our knowledge other *O*-glycoside-based multivalent constructs – many known to interact potently with lectins – have not yet been evaluated as putative inhibitors of glycosidases, although multivalent iminosugar analogs have been extensively studied in recent years.[54, 55] It is reasonable to expect that the novel phenomenon uncovered here may not be limited solely to glyco-ND but likely manifested by other multivalent constructs based on alternate scaffolds, NP-based or otherwise. The preliminary nature of the mechanism-of-inhibition proposed, here for α-*O*-glucosides and α-*O*-mannosides investigated herein makes it hazardous to speculate as to whether other *O*-glycosides might inhibit glycosidase action when presented multivalently on appropriate scaffolds.

The findings reported herein promise to impact on our understanding of the mechanisms-of-action of glycosyl hydrolases (and possibly those of other catalytic proteins) and will undoubtedly provide new opportunities for the design of synthetic enzyme inhibitors. The possibility that a multivalent ligand designed to modulate a selected lectin-ligand interaction might show cross-reactivity with one or more glycosidase, would seem to further complicate the development of multivalent compounds as therapeutic agents. Moreover, should any native multivalent glycodisplay be shown to inhibit, and thereby modulate, glycosidase action *in vivo*, this would need to be taken into account when rationalising a wide range of key biological phenomena known to be sensitive to the presence of glycans.[56-58]

4. Conclusions

We describe in this study the unprecedented finding that α-D-*O*-glucosides as well as α-D-*O*-mannosides when grafted

Acknowledgements

Notes

[a] Laboratoire de Glycochimie des Antimicrobiennes et Bioreseources, FRE 3517, Université de Picardie Jules Verne, 80039 Amiens, France; e-mail: aloysius.siriwardena@u-picardie.fr
[b] Institute of Electronics, Microelectronics and Nanotechnology (IEMN), UMR-CNRS 8520, Lille1 University, Avenue Poincaré-BP 60069, 59652 Villeneuve d'Ascq, France; e-mail: sabine.szunerits@iri.univ-lille1.fr
[c] Faculty of Chemistry, University of Sevilla, C/ Profesor Garcia Gonzalez 1, E-41012 Sevilla, Spain; e-mail: mellet@us.es
[d] Instituto de Investigaciones Químicas (IIQ), CSIC – Universidad de Sevilla, Avda. Américo Vespucio 49, E-41092 Sevilla, Spain; e-mail: jogarcia@iiq.csic.es

References

1 H. Hevey, L. Chang-Chun, *Adv. Carbohydr. Chem. Biochem.* , 2013, 125, 125.
2 T.R. Branson, T.E. McAllister, J. Garcia-Hartjes, M.A. Fasciones, J.F. Ross, S.L. Warriner, T. Wennekes, H. Zuilhof, W.B. Turnbull, *Angew. Chem. Int. Ed.*, 2014, 53, 8323.
3 T.K. Dam, T. A. Gerken, C. F. Brewer, *Biochem.*, 2009, 48, 3822.
4 E. Fan, Z. Zhang, W.E. Minke, Z. Hou, C.L.M. J. Verlinde, W.G.J. Hol, *J. Am. Chem. Soc.*, 2000, 122, 2663.
5 C. Fasting, C. A. Schalley, M. Weber, O. Seitz, S. Hecht, B. Koksch, J. Dernedde, C. Graf, E.-W.Knapp, R. Haag, *Angew. Chem. Int. Ed.*, 2012, 5, 10472.
6 P.I. Kitov, J.M. Sadowska, G. Mulvey, G.D. Armstrong, H. Ling, N.S. Pannu, R.J. Read, D.R. Bundle, *Nature*, 2000, 403, 669.
7 J.J. Lundquist, E.J. Toone, *Chem. Rev.*, 2002, 102, 555.
8 K.-F. Mo , T. Fang , S. H. Stalnaker , P. S. Kirby , M. Liu , L. Wells , M. Pierce , D. H. Live , G.-J. Boons, *J. Am. Chem. Soc.*, 2011, 133, 14418.
9 G.T. Nobel, F.L. Craven , J. Voglmeir , R. Šardzík , S.L. Flitsch, S.J. Webb *J. Am. Chem. Soc.*, 2012, 134, 13010.
10 C.M. Payne, W. Jiang, M. R. Shirts, M. E. Himmel, M. F. Crowley, G. T. Beckham, *J. Am. Chem. Soc.* , 2013, 135, 18831.
11 Z. Wang, Z. S. Chinoy, S. G. Ambre, W. Peng, R. McBride, R. P. de Vries, J. Glushka, J. C. Paulson, G. J. Boons, *Science*, 2013, 341, 379.
12 V. Wittmann, R.J. Pieters, *Chem. Soc. Rev.* , 2013, 42, 4492.
13 B.T. Houseman, M. Mrksich, *Angew Chem Int Ed*, 1999, 38, 782.
14 A. Bernardi, J. Jiménez-Barbero, A. Casnati, C. De Castro, T. Darbre, F. Fieschi, J. Finne, H. Funken, K.-E. Jaeger, M. Lahmann, T.K. Lindhorst, M. Marradi, P. Messner, A. Molinaro, P.V. Murphy, C. Nativi, S. Oscarson, S. Penads, F. Peri, R.J. Pieters, O. Renaudet, J.-L. Reymond, B. Richichi, J. Rojo, F. Sansone, C. Schäffer, W.B. Turnbull, T. Velasco-Torrijos, S. Vidal, S. Vincent, T. Wennekes, H. Zuilhof, A. Imberty, *Chem. Soc. Rev.*, 2013, 42, 4709.
15 T.M. Gloster, D.J. Vocadlo, *Nat. Chem. Biol.*, 2012, 8, 683-669.
16 R.J. Nash, A. Kato, C.Y. Yu, G.W.J. Fleet, *Future Med. Chem*, 2011, 3, 1513-1521.
17 A.E. Stütz, T.M. Wrodnigg, *Adv. Carbohydr. Chem. Biochem.*, 2011, 66, 187-298.
18 A. Barras, F.A. Martin, O. Bande, J.S. Baumann, J.-M. Ghigo, R. Boukherroub, C. Beloin, A. Siriwardena, S. Szunerits, *Nanoscale*, 2013, 5, 2307.
19 M. Khanal, F. Larsonneur, V. Raks, A. Barras, J.-S. Baumann, F. Ariel Martin, R. Boukherroub, J.-M. Ghigo, C. Ortiz Mettet, V.

20 M. Khanal, T. Vausselin, A. Barras, O. Bande, K. Turcheniuk, M. Benazza, V. Zaitsev, C.M. Teodurescu, R. Boukherroub, A. Siriwardena, J. Dubuisson, S. Szunerits, *ACS Appl. Mater. Interfaces*, 2013, 5, 12488.
21 R. Martin, M. Alvaro, J.R. Herance, H. Garcia, *ACS Nano*, 20110, 4, 65.
22 I. Rehor, Slegerova, J. J.Kucka, V. Proks, V. Petrakova, M.-P. Adam, F. Treussart, S. Turner, S. Bals, P. Sacha, M. Ledvina, A.M. Wen, N.F. Steinmetz, P. Cigler, *Small*, 2014, 10, 1106.
23 J. Slegerova, M. Hajek, I. Rehor, F. Sedlak, J. Stursa, M. Hruby, P. Cigler, *Nanoscale*, 2015, 7, 415.
24 J. Wehling, R. Dringer, R.N. Zare, M. Maas, K. Rezwan, *ACS Nano*, 2014, 8, 6475.
25 V. Turcheniuk, V. Raks, R. Issa, I.R. Cooper, P.J. Cragg, R. Jijie, N. Dumitrescu, L.I. Mikhalovska, A. Battas, V. Zaitsev, R. Boukherroub, S. Szunerits, *Diam. Rel.Mater.*, 2015, http://dx.doi.org/10.1016/j.diamond.2014.12.002.
26 L. Marcon, F. Riquet, D. Vicogne, S. Szunerits, J.-F. Bodart, R. Boukherroub, *J. Mater. Chem.* , 2010, 20, 8064.
27 A.M. Schrand, H. Huang, C. Carlson, J.J. Schlager, E. Osawa, S.M. Hussain, L. Dai, *J. Phys. Chem. B*, 2007, 111, 2.
28 S.-J. Yu, M.-W. Kang, H.-C. Chang, K.-M. Chen, Y.-C. Yu, *J. Am. Chem. Soc.*, 2005, 127, 17604.
29 M. Khanal, V. Raks, R. Issa, V. Chernyshenko, A. Barras, J.M. Garcia Fernandes, A. Siriwardena, I. Cooper, P. Cragg, L.I. Mikhalovska, V. Zaitsev, R. Boukherroub, S. Szunerits, *Part. Part. Syst. Charact.*, 2015, DOI: 10.1002/ppsc.201500027.
30 M. Hartmann, P. Betz, Y. Sun, S.H. Gorb, T.K. Lindhorst, A. Krueger, *Chem. Eur. J.,*, 2012, 18, 6485.
31 B. Arribas , E. Suárez-Pereira , C. Ortiz Mellet, J.M. García Fernández, C. Buttersack , M.E. Elena Rodríguez-Cabezas , N. Garrido-Mesa , E. Bailon, E. Guerra-Hernández, A. Zarzuelo, J. Gálvez *J. Agric. Food Chem.* , 2010, 58, 1777.
32 D.A. Giljohann, D.S. Seferos , P.C. Patel , J.E. Millstone, N.L. Rosi, C.A. Mirkin, *Nano Lett.*, 2007, 7, 3818.
33 I. Papp, C. Sieben, K. Ludwig, M. Roskamp, C. Bottcher, S. Schlecht, A. Hermann, R. Haag, *Small*, 2010, 6, 2099.
34 R. Rísquez-Cuadro, J.M. García Fernández, J.-F. Nierengarten, C. Ortiz Mellet, *Chem. Eur. J.*, 2013, 19, 16791.
35 A.G. Barrientos, J.M. de la Fuente, M. Jiménes, D.C. Solis, F. J. , M. Martin-Lomas, S. Penades, *Carbohydr. Res.*, 2009, 344, 1474.
36 M. Moros, B. Hernáez, E. Garet, J.T. Dias, B. Sáez, V. Grazú, A. González-Fernández, C. Alonso, J.M. de la Fuente, *ACS Nano*, 2012, 6, 1565.
37 M. Moros, B. Pelaz, P. López-Larrubia, M.L. García-Martin, V. Grazú, J.M. de la Fuente, *Nanoscale*, 2010, 2, 1746.
38 V.M. Díaz Pérez, M.I. García-Moreno, C. Ortiz Mellet, J. Fuentes, J.C. Díaz Arribas, C.F. J., J.M. García Fernández, *J. Org. Chem.* , 2000, 65, 136.
39 E.M. Sánchez-Fernández, R. Rísquez-Cuadro, C. Ortiz Mellet, J.M. García Fernández, P.M. Nieto, J. Angulo, *Chem. Eur. J.*, 2012, 18, 8527.
40 R.A. Field, A.H. Haines, *Bioorg. Med.Chem Lett.*, 1991, 1, 661.
41 H. Bharathkumar, M.S. Sundaram, S. Jagadish, S. Paricharak, M. Hemshekhar, D. Mason, K. Kemparaju, K.S. Girish, Basappa, A. Bender, K.S. Rangappa, *PLOS ONE*, 2014, 9, e102759.
42 J. Castilla, R. Rísquez, D. Cruz, K. Higaki, E. Namba, K. Ohno, Y. Suziki, Y. Díaz, C. Ortiz Mellet, J.M. García Fernández, S. Castillón, *J. Med. Chem.*, 2012, 55, 6857.
43 J.M. de la Fuente, A.G. Barrientos, T.C. Rojas, J. Rojo, J. Canada, A. Fernandez , S. Penades, *Angew Chem Int Ed*, 2001, 40, 2257.
44 N.C. Reichardt, M. Martin-Lomas, S. Penades, *Chem. Soc. Rev.*, 2013, 42, 4358.
45 M.B.S. Thygesen, J., K.J. Jensen, *Chem. Eur. J.*, 2009, 15, 1649.
46 S. Thobhani, B. Ember, A. Siriwardena, G.-J. Boons, *J. Am. Chem. Soc.*, 2003, 125, 7154.
47 A.B. Boraston, D.N. Bolam, H.J. Gilbert, G.J. Davies, *Biochem. J.*, 2004, 382, 769.
48 H.J. Gilbert, *Plant. Physiol.*, 2010, 153, 444.
49 D. Guillén, S. Sánchez, R. Rodríguez-Sanoja, *App. Microbiol. Biotechnol.*, 2010, 85, 1241.
50 S. Cuyvers, E. Dornez, J.A. Delcour, C.M. Courtin, *Critical Reviews in Biotechnology*, 2012, 32, 93.
51 E.C. O'Neill, A. Rashid, C.E.M. Stevenson, A.-C. Hetru, A.P. Gunning, M. Rejzek, S. A. Nepogodiev, S. Bornemann, D. M. Lawson, R. A. Field, *Chem. Sci.*, 2014, 4, 341.

52 C. Ragunath, S.G. Manuel, V. Venkataraman, H.B. Sait, C. Kasinathan, N. Ramasubbu, *J. Mol. Biol.*, 2008, 384, 1232.
53 R.H. Jacobson, X.-J. Zhang, R.F. DuBose, B.W. Matthews, *Nature* 1994, 369, 761.
54 P. Compain, A. Bodlenner, 2014, 15, 1239.
55 S.G. Gouin, *Chem. Eur. J.*, 2014, 20, 11616.
56 J.W. Dennis, C.F. Brewer, *Mol Cell Proteomics*, 2013, 12, 913.

57 A. Varki, R. D.Cummings, J. D. Esko, H. H. Freeze, P. Stanley, C. R. Bertozz, G. W. Hart, M. E. Etzler, Essentials of Glycobiology, Cold Spring Harbor Laboratory Press, Cold Spring Harbor, NY, 2009.
58 B. Wang, B. G-J, Carbohydrate Recognition: Biological Problems, Methods, and Applications., John Wiley & Sons, Hoboken, 2011.